ESO-74-B
July 1998

Scientific simulations on the VLT interferometer

M. Schöller, C. Denise, and B. Koehler

European Southern Observatory
85748 Garching b. München, Germany

FERMILAB
SEP 17 1998
LIBRARY

ABSTRACT

By the middle of the year 2000 the VLT interferometer will become operational. The design of the telescopes, Coudé trains and delay lines is finished and the different beam combination instruments for use in the near and mid infrared are under design. Our goal is to understand this complex machine in full detail and analyze the influence of the several subsystems on the data formation process. ESO has already started to model the interferometer from an optomechanical point of view which resulted in the VLTI end-to-end model. The end-to-end model includes the complete optical trains for the 4 unit telescopes and up to 4 auxiliary telescopes located on any of the 30 telescope stations. The optical trains consist of 16 mirrors from the primary mirror to the beam combination lab. The model also includes seismic noise, wind load, atmospheric effects, delay line control, fringe sensor unit, and fast image stabilization. The output of this model enters the scientific simulations, where the beam combination instruments are modeled. We will explain the underlying philosophy of our model and show first illustrations from the simulations.

Keywords: Interferometry, VLTI, Simulation, Model, Very high angular resolution

ESO-74-B

1. INTRODUCTION

The Very Large Telescope (VLT) is under construction on Cerro Paranal in the Atacama desert, about 100 km south of Antofagasta in Chile. It consists of four 8 m unit telescopes (UTs) and relocatable 1.8 m auxiliary telescopes (ATs), which can be put on thirty telescope stations. The unit telescopes will be used as ordinary single dish instruments with their own astronomical instruments, but from the start of the design it was foreseen to combine the four telescopes into the Very Large Telescope Interferometer (VLTI). In the first phase VLTI will combine two UTs, later two ATs, with the possibility to combine more telescopes in the future. The space in the delay line tunnel can hold up to eight delay lines. Figure 1 shows the layout of the VLTI. The progress of the work on Paranal can be seen in figure 2. An overview of the scientific and technical aspects of VLTI can be found in several publications[1,2,3] . The instruments which are used at VLTI are not built by ESO itself but by several institutes of the interferometric community in Europe. There are two instruments foreseen early in operations: AMBER[4] , an instrument which will start observing in the near infrared, with the possibility to observe down to 600 nm with the ATs. AMBER will accommodate up to three beams, making closure phase imaging possible, doing beam combination in the image plane. It also provides spectroscopic capabilities. MIDI[5] will observe at 10 μm, with the possible extension to 20 μm, combining two beams in the pupil plane. PRIMA[6] is a further instrument which may become a facility within the interferometer. PRIMA will provide phase referenced imaging in a first step and be able to perform microarcsecond astrometry in a second phase.

There are many reasons for us to simulate the behavior of the VLT interferometer and the observations that will be carried out with it and its instruments. Optical interferometry is a complex and complicated tool. The final information one wants to obtain is deeply embedded within the data observed. In the past several simulations of observations with the VLTI were carried out[7,8,9] , which all assume a certain behavior of the interferometer or a certain observation mode. Our aim is to simulate data which is as close to reality as possible, helping us to understand how the interferometer will be used for observations. We will discuss the need for a simulator in more detail in section 2. Section 3 gives an overview about the model, and in section 4 we describe the software we use in more detail. Then we have a look on what beam combination with an interferometer means (section 5), and finally we discuss what further efforts have to be done in the future (section 6) .

Email addresses: mschoell@eso.org, cdenise@eso.org, bkoehler@eso.org

Fermilab Library
0 1160 0067553 2

Figure 1. The layout of the VLT interferometer. The four UTs with their enclosures and the 30 AT stations can be seen. The AT stations are connected by rail tracks on which the ATs can be moved. Also shown are the delay line tunnel and the beam combination laboratory. Each AT station and all four UTs are lying on the intersections of a 8x8 m grid, which rests in the indicated *uv*-frame, tilted by 19.55 degrees to the north.

2. MOTIVATION

The main objective of the science simulator development is to determine realistic VLTI capabilities. Interferometry is too complex to be characterized by standard parameters and the instrument's response depends intimately on the source characteristics. Thus we have to create a tool which incorporates all important aspects of the interferometer, taking the astronomical object into account, and producing data as close to reality as possible. As with every astronomical project we have to maximize the operational efficiency for optimal scientific results. To achieve this we have to compute the optimal observing configuration, exposure time, and observing mode for the expected source parameters. We also want to check if the goals set by the science drivers can be reached. Furthermore we want to establish precise testing and calibration requirements. It will also be important to establish optimal data analysis procedures and pipeline processing. It will be necessary to check existing software packages and algorithms to work on the data taken, adapt these, or code new software. We also have to assess the impact of design changes on the science output. We have to study the confidence level and precision of results versus technical and cost trade-offs and solutions (e.g. mirror coatings, styrofoam insulation, discontinuous delay line operations, siderostat diameter, AT designs). And finally we want to allow smart, useful, and friendly VLTI-user interaction. The simulator will be available to operators, proposers, and instrument teams to plan and execute observations, especially in competition for time at the UTs with single dish experiments.

3. MODEL PHILOSOPHY

When starting to build the science model in summer 1997 we already had a working technical end-to-end model written in MATLAB/SIMULINK which includes all the details of optics, mechanics, distortions, etc. We didn't want to build the science simulator into this model since it would not make use of the SIMULINK capabilities, but aimed

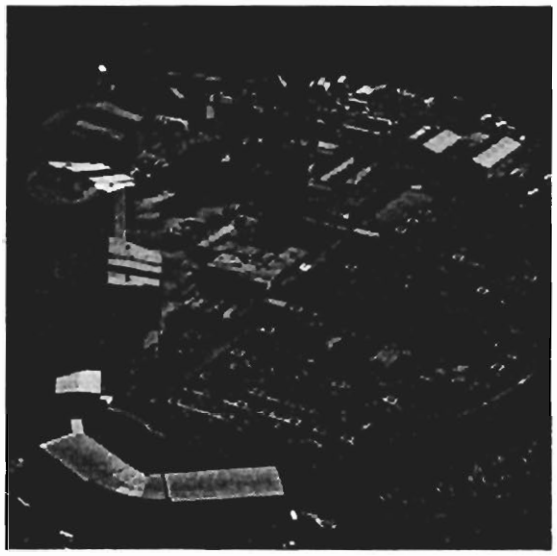

Figure 2. The Paranal site under construction on December 16, 1997. On the left the enclosures of UT1, UT2, and UT3 can be seen. In the background UT4 is still under construction. Running diagonally through the picture is the delay line tunnel. Close to it the beam combination building and most of the foundations for the 30 AT stations can be seen. In the foreground on a lower level the control building is located.

at high speed. A lot of its features would also be used later for observers in a UNIX environment, complying with ESO standards. On the other hand we wanted to use all features provided by the technical model for the science simulations. This let us come up with the scheme displayed in figure 3.

Beside the technical characteristics and the disturbance parameters, the technical model is also influenced by some of the object characteristics like the position on the sky, magnitude at various wavelengths, visibility at a given baseline, and the configuration of the VLTI. One of the results from the technical model are the wavefronts for every arm of the interferometer and every sampling step (e.g. 5 ms). These wavefronts are then used inside the science model together with other aspects of the astronomical source and the interferometer configuration. Within the science model the beam combination is done. This takes also into account observation mode, observation sequence, and exposure time, and finally leads to simulated raw data.

4. THE SCIENCE SIMULATOR SOFTWARE

4.1. The Technical End-to-End Model

The development of the VLTI End-to-End Model[10] started in June 1996. The main objective of the model is to produce a representation of the main output of the interferometer. This is the intensity produced by the superposition of the electromagnetic fields collected by the elements of the interferometric array. The superposition shall be done either in the pupil plane conjugate or in an image plane along a single line of sight (point source on-axis).

The model is developed for engineering purposes in the MATLAB 5.1 / SIMULINK 2.1 environment under Windows NT with the following objectives:

- Analyze collective effects of disturbances in the time domain
- Analyze interaction of optics and control loops including cross-coupling between the various tracking loops
- Validate and maintain the main VLTI error budgets
- Study design alternatives when necessary and when having high impact at system level (e.g. UT Coudè Train, Dual Feed mode, etc.)

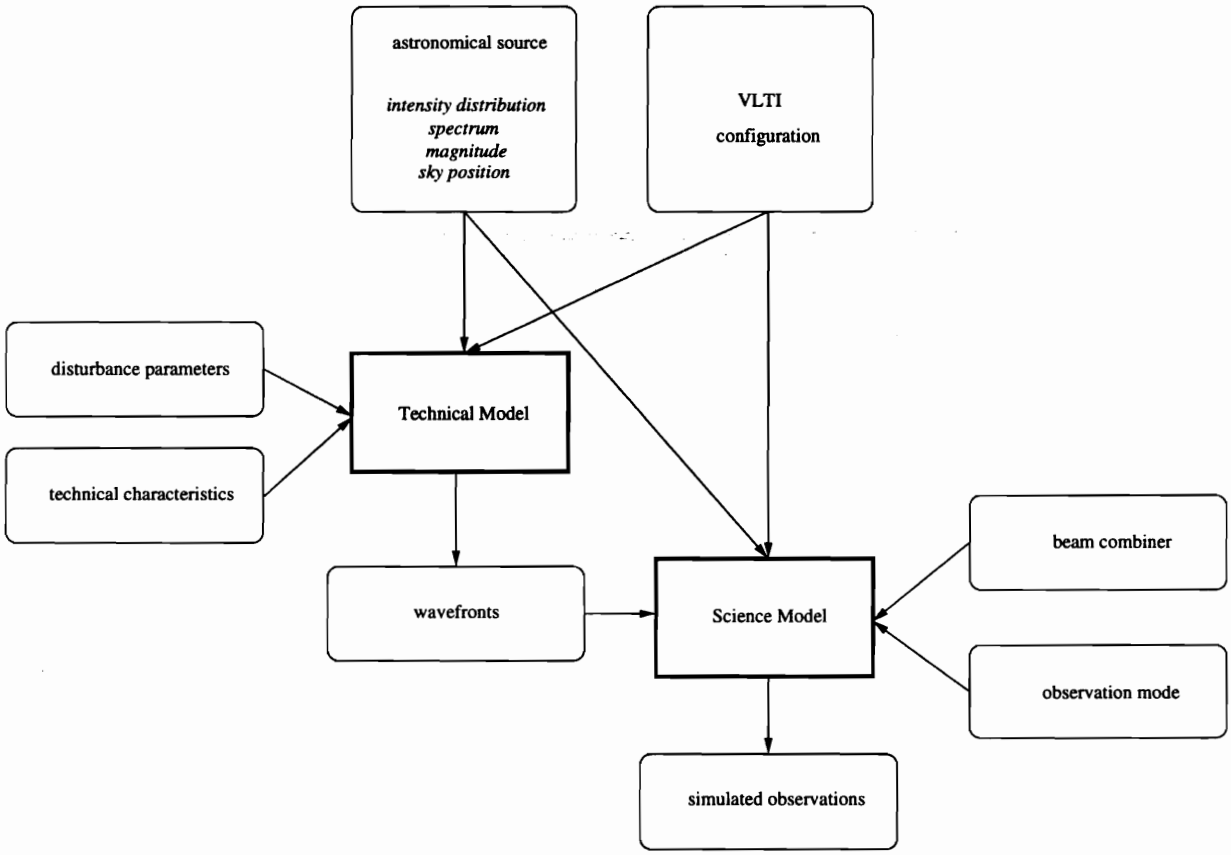

Figure 3. Schematic overview of the philosophy of the science model for the VLTI (see text).

Within the model a global ray-tracing is performed and a sensitivity matrix is computed. Various noise sources like atmospheric, wind, or seismic, are generated and fed through mechanics and optics. Noise is applied to the detectors which feed the different control loops. Also the delay line position and the zoom mirror curvature are determined. The simulation itself runs with the full SIMULINK capabilities and computes the position of the output pupil and a description of the electromagnetic field within the output pupil for up to four beams and every sampling step. The features of the technical model can be found in table 1.

Figure 4 shows a result of the ray tracing performed with the end-to-end model. The expected visibility degradation introduced by the interferometer is displayed in figure 5. In figure 6 you can see the phase within two output pupils for one time step as calculated by the end-to-end model after conversion in the science model software.

4.2. The image processing software

The image processing software used with the science simulator performs all time consuming tasks necessary for the formation of fringes. These tasks are mainly conversion of Zernike polynomials into phase maps, Fourier transforms, and averaging over the exposure time.

This software package consists of about 25 single programs coded in C++ which can be roughly divided into three different types: image manipulation programs, conversion programs, and beam combination programs.

Except for the more complex beam combination programs every program performs a small task, being powerful when combined together. The image format used is FITS *, all other data is exchanged in ASCII. The programs

*http://www.cv.nrao.edu/fits/

	Ready in 1.2	Foreseen in 2.0	Future features
Optics	Build-in Ray Tracing: flat, cylindric, spheric, conic mirrors "Perfect" surfaces, Prescription errors but no figuring errors 5 DOF's per mirror: X, Y, Z, α, β	Photometry Figuring errors Polarization	Full Diffraction Dispersion
Mechanics	Linear models: Frequency response (FR) or State Space representation (SS) FR or SS computed before-hand by FEM, and loaded from file		Direct interface with FEM Built-in Finite Element capabilities
Control	Full SIMULINK capabilities Linear detector models (frequency response and noise) Linear control laws	Complete detector models	Mode Switching
Object	Point source with associated magnitude and visibility (for detectors) Monochromatic	Polychromatic	Extended Object
Sub-systems	4 Telescopes among 4 UTs and 30 AT stations 4 Delay Lines among 8 available Delay Lines incl. Variable Curvature Mirror Main Control Loops (Fast Tip/Tilt, Lateral Pupil Position, Fringe Tracking)		Adaptive Optics Dual Feed mode
Disturbances	Atmosphere (Piston, Tip/Tilt) Wind load on Telescope (Piston, Tip/Tilt) Seismic (Piston)	Atmosphere (Wave Front Error) Internal Seeing	
Output parameters	Computed in User-defined output plane For each beam: * Chief-Ray position X, Y, Z * Chief-Ray OPL * Pupil Position X, Y, Z * Phase Map (Zernike) * Image Position at Telescope coudé * Pupil diameters	Additional characteristics * Photometric * Polarization	

Table 1. Present and future features of the technical model. Features in the second column are present in the current version (1.2). The third column lists features which are being coded while this paper is written. The last column holds features which have to follow in a later version.

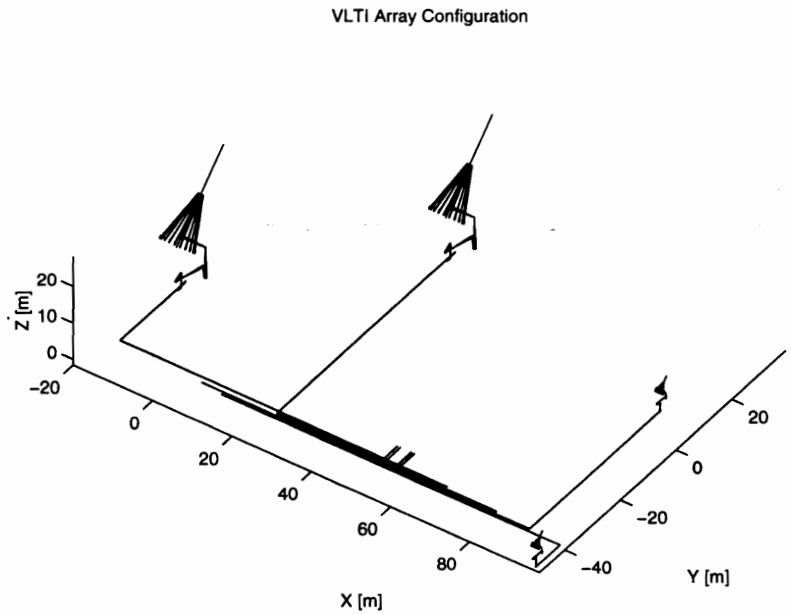

Figure 4. Ray tracing output from the end-to-end model. Shown are UT1 and UT2 accompanied by two ATs sitting on the AT stations named J3 and K0, pointing at 45° elevation angle towards the v-axis, which is tilted 19.55° to the north. For each telescope you can follow the rays starting at M1, going through the Coudè train, entering the delay line tunnel, being reflected in the cat's eyes of the delay lines and finally entering the interferometric lab. On top of each telescope there is an elongated chief ray attached to indicate the pointing direction.

themselves retrieve all commands via the command line and are able to read and write data via stdin and stdout, as well as read from and write to files. Because of this it is easy to use them in batch mode. Although it is possible to perform the beam combination exclusively with the modular programs, we decided to write two dedicated beam combiner programs for higher efficiency.

The software makes use of the following external libraries:

aips C++ file input/output library from the AIPS++ project to read and write FITS files. Allows to read from stdin and write to stdout and thus using the programs with pipes. †

images C++ library coded by Thorsten Reinheimer which defines real and complex image objects including a huge number of operations on them and thus makes coding, reading, and maintaining programs easier.

fftw-1.1 C library from the MIT to make efficient fast Fourier transforms. ‡

Options C++ library from Brad Appleton which enables command line parsing. §

4.3. The User Interface

The User Interface helps the user to perform the simulations in a guided and documentable way and is written in Tcl/Tk. For each simulation the parameters can be chosen and saved into a parameter file, which can also be edited by hand. Then the program generates one file per simulation in MATLAB format which supplies the technical model with all necessary input parameters. After these simulations are carried out by the technical model, the user just presses a button and the beam combination process runs automatically using the parameters given before. The

†http://aips2.nrao.edu/aips++/docs/html/aips++.html
‡http://theory.lcs.mit.edu/ fftw/
§http://www.enteract.com/ bradapp/ftp/src/libs/C++/Options.html

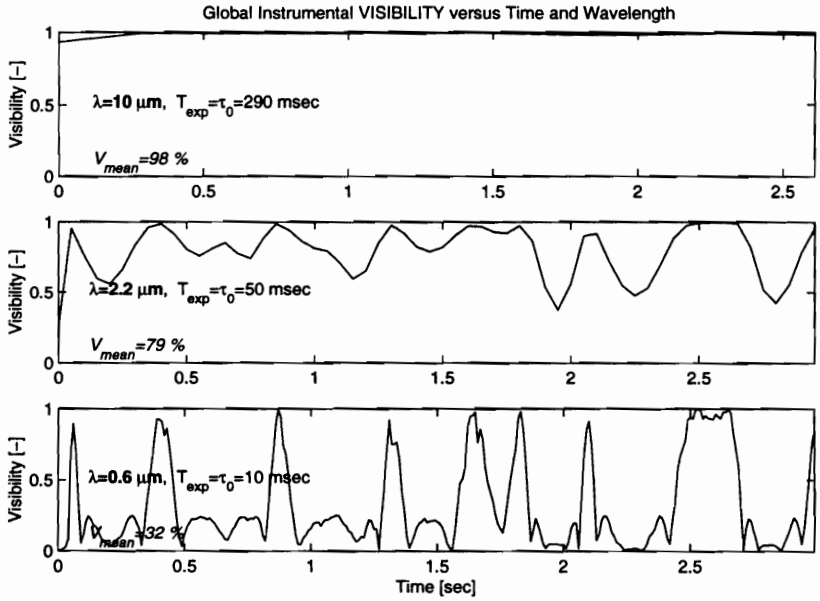

Figure 5. Global instrumental visibility as measured by an idealized pupil plane instrument. The visibility measured by a true instrument will be severely effected by thermal background at 10 μm and atmospheric wave front error at the shorter wavelengths which are both not modeled yet. The peaks with a period of $\frac{1}{2}$ second in the 0.6 μm visibilities come from the residual tracking errors of the telescopes under wind load, which lets the two airy disks overlap only from time to time. These residual errors can be corrected by increasing the gain of the fast tracking loop set to low values here on purpose. The first 100 ms of each time series are dominated by the model initialization phase and are not usable.

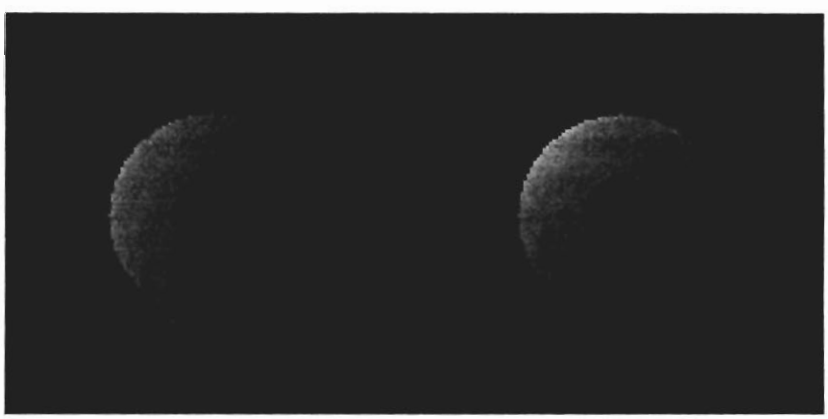

Figure 6. Phase within the output pupil for two arms of the interferometer.

simulation itself is carried out by calling the C++ beam combination programs. The science object can be built with a few standard models like binaries, stellar surfaces, and circumstellar disks, or put together from a small number of geometric bodies. Furthermore the user sets coordinates and magnitude for the object and selects the wavelength at which he wants to observe as well as hour angle interval and increment, and exposure time. Further parameters are the selection of beam combiner and spatial filtering. Once the simulation is finished, the user can extract the

visibilities he wanted to measure directly from the data. These are printed out to the screen. In a later version it is foreseen to produce LaTeX output which then can easily be compiled into a document.

Of course, the user also has to select the layout of the interferometer. From the 30 AT stations alone he can select between about 250 different baselines and more than 3000 different closures. The software checks this array configuration against boundary conditions (number of delay lines per side of mountain, number of ATs per track, shadowing of ATs by a UT enclosure, beam intersection by moving delay line). This check can also be performed without using the full science model. It is also possible to compute the uv-coverage of the interferometer for the chosen object coordinates, observation times, and interferometer layout.

5. BEAM COMBINATION

5.1. Imaging through an interferometer

Imaging through an optical system can be described by the incoherent space invariant imaging equation:

$$i(\mathbf{x}) = o(\mathbf{x}) * p(\mathbf{x}) \tag{1}$$

(where $i(\mathbf{x})$ denotes the intensity distribution of the image, $o(\mathbf{x})$ the intensity distribution of the object, $p(\mathbf{x})$ the point spread function, $\mathbf{x}$ a two dimensional vector in image space, and $*$ a convolution), or its Fourier transform:

$$I(\mathbf{u}) = O(\mathbf{u})P(\mathbf{u}) \tag{2}$$

(with $I(\mathbf{u})$, $O(\mathbf{u})$, $P(\mathbf{u})$ being the Fourier transforms of $i(\mathbf{x})$, $o(\mathbf{x})$, $p(\mathbf{x})$, $\mathbf{u}$ is a two dimensional vector in Fourier space. $P(\mathbf{u})$ is the modulation transfer function (MTF)).

If an interferometer is operating in Fizeau mode, you can easily apply the equations above and get an interferogram of the object you are observing, by taking only the entrance pupil of the interferometer into account when computing the MTF. In Michelson mode, which is used in most interferometers including VLTI, the object image relationship is somewhat more complicated[11] .

This is due to the fact that entrance and exit pupil of the optical system are not aligned in the same way. The entrance pupil of most earth bound interferometers is different for objects with different declinations and varies with time. Thus the part of the object complex visibility which is measured with the interferometer varies with time (see fig. 7). The exit pupil on the other hand usually does not vary with time. The spacing of the fringes one obtains with the interferometer depends only on the shape of the exit pupil, or better its autocorrelation, the MTF. The MTF for an image plane beam combination with two telescopes can be seen in figure 8. The MTF for a pupil plane beam combination is quite similar to the one in image plane mode. The three different parts of the MTF are on top of each other. This leads to a fringe separation of infinity. To measure the fringe one has to step through the fringe in time. This can be done by using a fast delay line which adds additional optical path to one of the beams.

Another problem of a Michelson interferometer is the limited field of view. This is due to the fact that a Michelson interferometer is not homothetic. Since the exit pupil is not a scaled down version of the entrance pupil, the interfering wavefronts are somewhat tilted. This means that outside a certain area the two wavefronts don't interfere with each other. A larger field of view can be achieved by getting a larger coherence length, i.e. using narrow wavelength bands.

5.2. Pupil plane (coaxial) beam combination

Most interferometers are combining the beams coming from the arms of the interferometer in the pupil plane. This means that the output pupils are aligned pairwise on top of each other. Afterwards usually an optic creates an image of this pupil on a detector.

To measure the fringe, the observer now has to step through the fringe in time, namely modulating the optical path in one of the beams. One way to achieve this in a fringe tracking interferometer is by taking four frames per coherence time interval, each of which has $(0,1,2,3)\times\frac{\lambda}{4}$ optical path difference (OPD) added to one beam. The visibility is estimated by determining the intensity in each of the four frames and computing the visibility according to: $\frac{1}{2}\sqrt{(A-C)^2+(D-B)^2}$. For the beam combination in the science model this means that you have to add 0, $\frac{\pi}{2}$, π, $\frac{3\pi}{2}$ to the phase in one of the off center MTF peaks, and subtract the same value in the other off center peak. This beam combination mode is foreseen with the MIDI instrument. Four typical interferograms can be seen in figure 9.

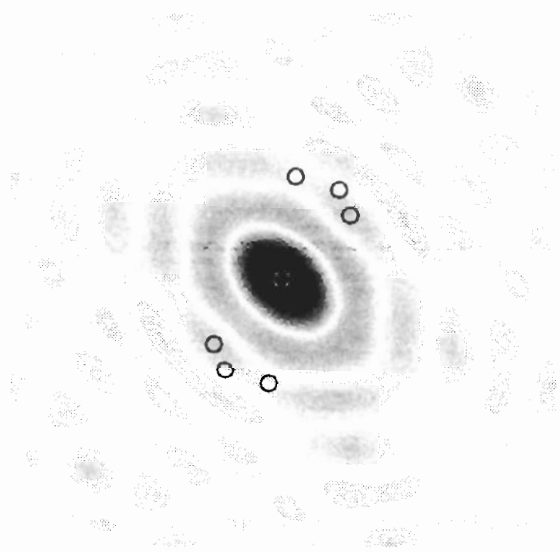

Figure 7. Modulus of the object complex visibility of a uniform ellipse. The encircled areas are the parts of the complex visibility picked up by UT1 and UT3 for an object at declination -30° and hour angles -3, 0, and 3.

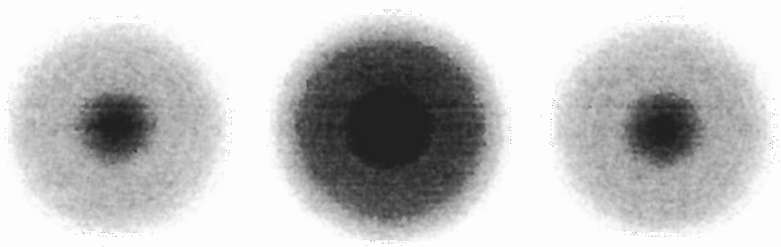

Figure 8. Modulation transfer function (MTF) for an image plane beam combiner. This is the autocorrelation of the phase of the electromagnetic waves at the output pupil. The structure of the MTF is mainly given by the autocorrelation of two uniform disks. Distortions from this shape come from the phase errors introduced by the interferometer and simulated in the technical end-to-end model.

5.3. Image plane (multiaxial) beam combination

When combining the interferometer's beams in the image plane, the output pupils of two or more arms of the interferometer are aligned beside each other in a pupil plane. Behind this plane the pupils are imaged to form fringes in space. The output pupils have to be aligned so there is no redundancy in the distances between them. Usually the output pupils are set on a line, with non redundant spacing, leaving the perpendicular axis available for spectroscopy. A more compact setup uses two dimensions, taking for example a trapezium structure with four output pupils.

In multiaxial mode one takes one frame per coherence time interval which shows fringes in space. For estimating the visibility, one has to perform a Fourier transform on the fringe and compute the ratio between the central peak and one of the side peaks. This mode will be used by the AMBER beam combiner. In figure 10 an image plane combined interferogram can be seen.

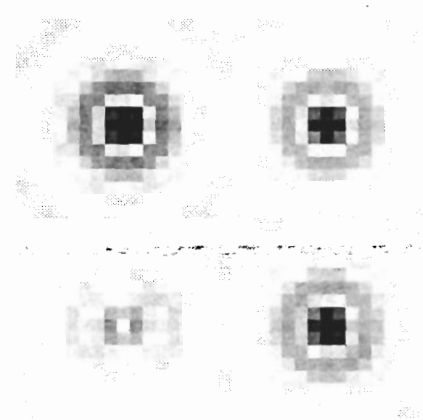

Figure 9. Pupil plane combined interferograms at $10\mu m$ for delays of 0, $\frac{\lambda}{4}$, $\frac{\lambda}{2}$, and $\frac{3\lambda}{4}$ (non-linear display). The lower left interferogram should be 0 over the whole image for a perfect interferometer and an unresolved object. This is not the case because of a non-zero optical path difference (OPD) between the two arms of the interferometer and different distortions in the optics.

Figure 10. Image plane combined interferogram at $2\mu m$. One can see the fringes within the airy disk including the first diffraction ring. The airy disk is squeezed since it is not necessary to sample it perpendicular to the fringes.

5.4. Illustrations from the model

At the moment of writing this paper we are not yet at the stage to perform science simulations which are as close to reality as we would like them to be. Because of this we don't want to discuss science results but just show the effects that disturbances and limitations will have on the raw data and the derived values.

As has already been lined out in the caption to figure 5 residual tilt is dominating the degradation of the visibility at short wavelengths. In figure 11 the residual tilt is shown with the same degree of distortions, but for different wavelengths. While for 10 μm the airy disks overlap perfectly, at 2 μm one can see a slight elongation, and for 500 nm the airy disks are separated.

Another aspect we want to study is the influence of the detector and using the interferometer at low light levels. We added noise to an image plane combined interferogram, corresponding to 10,000 photons and 20 e^- readout noise. In figure 12 the modulus of the corresponding Fourier spectrum can be seen in a non-linear display. The off-peaks which carry the signal we want to measure can hardly be seen, thus degrading the visibility immensely.

6. OUTLOOK

There are several things which have to be done in the simulation of raw data. First it will be necessary to include adaptive optics phase maps in the model to be able to simulate observations in the near infrared with the UTs. Then

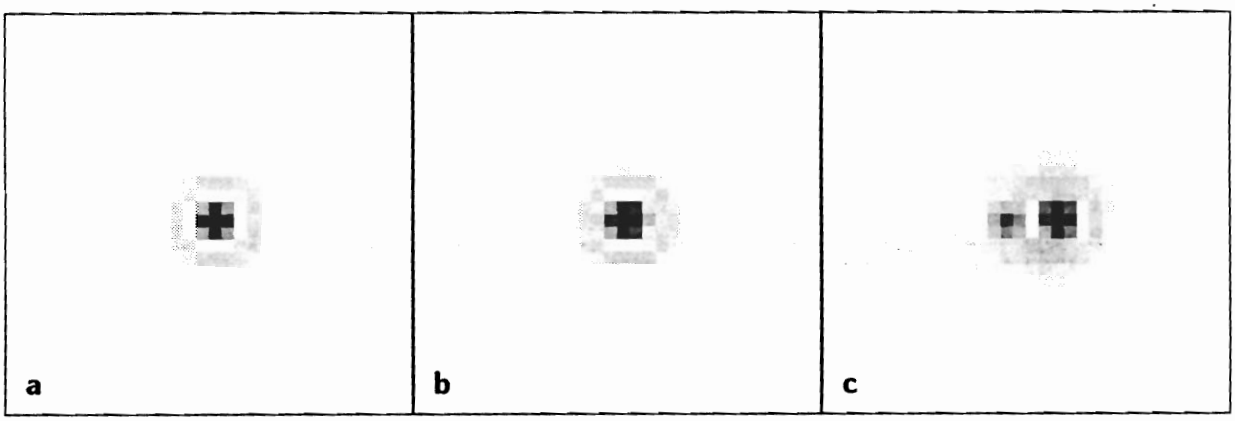

Figure 11. Pupil plane combined interferograms at **a** $10\mu m$, **b** $2\mu m$ and **c** $500nm$ (see text).

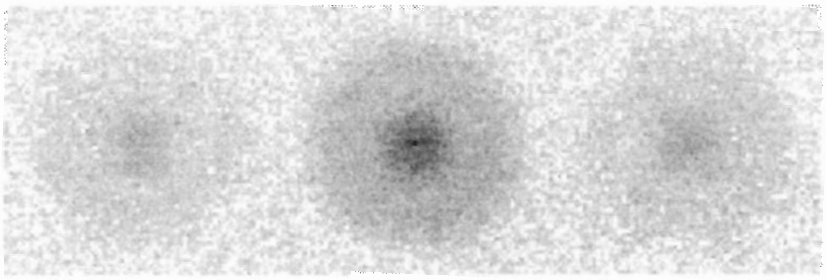

Figure 12. Fourier spectrum of an image plane combined interferogram at $2\mu m$ with 10,000 photons and 20 e^- readout noise (non-linear display).

it will be important to determine the noise coming from the beam combination instruments (background, detector, etc.) in close cooperation with the instrument consortia. Also the visibility loss due to spectral bandwidth has to be calculated and the beam combination must also provide spectral resolution. A further task for the simulation will be multiple beam image plane recombination, including different setups for the output pupils.

And finally we have to put together, adapt, and code software packages for image modeling and reconstruction. Here we hope to get input from already existing optical interferometers and the superb experience within the European radio interferometry community, as well as making use of rapidly advancing software products (e.g. AIPS++[12]).

REFERENCES

1. F. Paresce, D. Mourard, T. Bedding, J. Beletic, C. Haniff, C. Leinert, F. Malbet, J.-M. Mariotti, D. Mozurkewich, R. Mundt, P. Petitjean, A. Quirrenbach, T. Reinheimer, A. Richichi, H. Rottgering, O. von der Lühe, and R. Waters, "A new start for the VLTI," *ESO Messenger* **83**, pp. 14–21, 1996.
2. O. von der Lühe, D. Bonaccini, F. Dérie, B. Koehler, S. Levêque, E. Manil, A. Michel, and M. Verola, "A new plan for the VLTI," *ESO Messenger* **87**, pp. 8–14, 1997.
3. J.-M. Mariotti, C. Denise, F. Dérie, M. Ferrari, A. Glindemann, B. Koehler, S. Levêque, F. Paresce, M. Schöller, M. Tarenghi, and M. Verola, "The VLTI program: a status report," in *Astronomical Interferometry*, R. D. Reasenberg and J. B. Breckinridge, eds., *Proc. SPIE* **3350**, 1998.
4. F. Malbet, G. Perrin, R. Petrov, A. Richichi, and M. Schöller, "AMBER - The imaging and spectroscopic VLTI focal instrument," Preliminary study for the ESO Interferometric Science Advisory Committee (ISAC), 1997.
5. C. Leinert and U. Graser, "MIDI: a mid-infrared interferometric instrument for the VLTI," in *Astronomical Interferometry*, R. D. Reasenberg and J. B. Breckinridge, eds., *Proc. SPIE* **3350**, 1998.

6. A. Quirrenbach, V. C. du Foresto, G. Daigne, K.-H. Hofmann, R. Hofmann, R. L. Poole, D. Queloz, and F. Vakili, "PRIMA: a study for a dual-beam instrument for the VLTI," in *Astronomical Interferometry*, R. D. Reasenberg and J. B. Breckinridge, eds., *Proc. SPIE* **3350**, 1998.
7. T. Reinheimer, K.-H. Hofmann, and G. Weigelt, "Interferometric imaging with arrays of large optical telescopes in the multi-speckle mode," *A&A* **279**, pp. 322–334, 1993.
8. F. Malbet and C. Bertout, "Detecting T Tauri disks with optical long-baseline interferometry," *A&AS* **113**, p. 369, 1995.
9. N. Ageorges and O. von der Lühe, "Simulations of VLTI/VISA imaging observations of young stellar objects at 2.2 μm," *ESO Messenger* **85**, pp. 18–22, 1996.
10. C. Denise and B. Koehler, "VLTI End-to-End model user guide," Tech. Rep. VLT-MAN-ESO-15000-1569, European Southern Observatory, 1998.
11. M. Tallon and I. Tallon-Bosc, "The object-image relationship in Michelson stellar interferometry," *A&A* **253**, pp. 641–645, 1992.
12. G. A. Croes, "On AIPS++, A New Astronomical Information Processing System," in *Astronomical Data Analysis Software and Systems II*, R. J. Hanisch, R. J. V. Brissenden, and J. Barnes, eds., *A.S.P. Conference Series* **52**, p. 156, 1993.

NAME | I D No. | M.S.

RETURN TO FERMILAB LIBRARY